

## Measuring Site-Specific Cluster–Surface Bond Formation

Regina Hoffmann,\* Clemens Barth, Adam S. Foster, Alexander L. Shluger, Hans J. Hug, Hans-Joachim Güntherodt, Risto M. Nieminen, and Michael Reichling

Contribution from the Physikalisches Institut, Universität Karlsruhe, Wolfgang-Gaede-Str. 1, 76128 Karlsruhe, Germany, CRMCN-CNRS, Campus de Luminy Case 913, 13288 Marseille Cedex 09, France, Laboratory of Physics, Helsinki University of Technology, P.O. Box 1100, 02015 HUT, Finland, Department of Physics and Astronomy, University College London, Gower Street, London WC1E 6BT, United Kingdom, Swiss Federal Laboratory for Materials Testing and Research, CH-8600 Dübendorf, Switzerland, NCCR Nanoscale Science, Universität Basel, Klingelbergstrasse 82, 4056 Basel, Switzerland, and Fachbereich Physik, Universität Osnabrück, Barbarastrasse 7, 49076 Osnabrück, Germany

Received August 12, 2005; E-mail: r.hoffmann@pi.uka.de

**Abstract:** Recent advances in dynamic force microscopy show that it is possible to measure the forces between atomically sharp tips and particular atomic positions on surfaces as a function of distance. However, on most ionic surfaces, the positive and negative ions can so far not be distinguished. In this paper, we use the  $\text{CaF}_2(111)$  surface, where atomic resolution force microscopy has allowed identification of the positions of the  $\text{Ca}^{2+}$  and  $\text{F}^-$  ions in the obtained images, to demonstrate that short-range interaction forces can be measured selectively above *chemically identified* surface sites. Combining experimental and theoretical results allows a quantification of the strength and distance dependence of the interaction of a tip-terminating cluster with particular surface ions and reveals details of cluster and surface relaxation. Further development of this approach will provide new insight into mechanisms of chemical bond formation between clusters, cluster deposition at surfaces, processes in adhesion and tribology, and single atom manipulation with the force microscope.

## Introduction

The analysis, creation, and manipulation of individual nanostructures is most often accomplished by approaching the structure with the atomically sharp tip of a scanning probe microscope. For the investigation of dielectric nanosystems with utmost resolution, the dynamic scanning force microscope (SFM) is used.<sup>1,2</sup> The force acting on the tip during approach of the investigated object is composed of several contributions of various strength and distance dependence,<sup>3</sup> as illustrated in the schematic force curve shown in Figure 1a. High-resolution dynamic SFM in the so called noncontact mode is operated in the regime of attractive total force with a set-point very close to the minimum of the force curve. Here, we are interested in chemical interactions, namely, forces acting between only a few atoms at the tip end, referred to here as the *tip-terminating cluster*, and individual ions of a dielectric surface. These forces have a decay length on the order of 0.1 nm (region II in Figure 1a), while long-range forces, such as van der Waals and electrostatic forces, act on the entire tip apex over tens of nanometers (region III in Figure 1a). By fitting an appropriate interaction model to the measured force curve, we can deduce long-range force contributions as shown in Figure 1b for the  $\text{CaF}_2(111)$  surface studied here. These data are used to extract

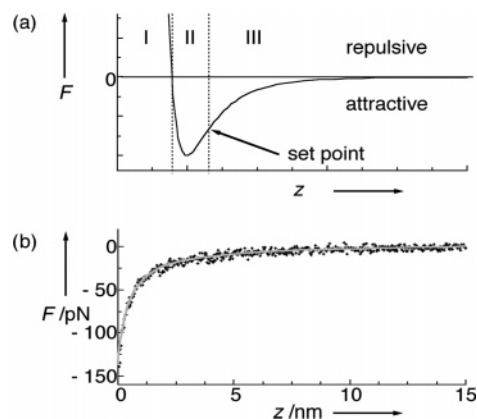


**Figure 1.** (a) Schematic illustration of the dependence of the total force on the tip–surface distance in force microscopy. Three regions of tip–surface interaction can be identified: (I) short-range repulsion (not relevant in the context of this work), (II) short-range attraction (chemical forces yielding atomic contrast), and (III) long-range attractive interaction (van der Waals and electrostatic forces). For atomic resolution imaging, the dynamic force microscope is operated in the regime of attractive interaction, where the gradient of the total force is positive but very close to the minimum of the force curve (set point). (b) Measurement of long-range interaction forces on the  $\text{CaF}_2(111)$  surface (black dots) shown together with a fitted curve (grey solid line) obtained from simulation.

chemical forces at specific surface sites that are the focus of this work. The site-specific chemical interaction extracted from experiments is interpreted by comparison to results from sophisticated theoretical calculations based on several models for the tip-terminating cluster.

(1) García, R.; Pérez, R. *Surf. Sci. Rep.* **2002**, *47*, 197.

(2) Giessibl, F. J. *Rev. Mod. Phys.* **2003**, *75*, 949.

(3) Guggisberg, M.; Bammerlin, M.; Loppacher, C.; Pfeiffer, O.; Abdurixit, A.; Barwich, V.; Bennewitz, R.; Baratoff, A.; Meyer, E.; Güntherodt, H. *J. Phys. Rev. B* **2000**, *61*, 11151.

## Experimental Details and Details of the Calculation Methods

Experiments were performed with a home-built low-temperature force microscope described in detail previously.<sup>4</sup> Operation at cryogenic temperatures provides utmost stability, which is essential for measuring force curves above well-defined surface sites.<sup>5</sup> We chose the  $\text{CaF}_2$ -(111) surface for our studies since this binary material provides sites of distinctly different chemical characteristics, and topographic images yield characteristic contrast patterns that have been documented and fully interpreted in previous studies.<sup>6</sup> This allows us to unambiguously claim the chemical identity of all image features directly from an analysis of measured image patterns and scan lines even if the atomic structure of the tip apex changes.

A commercial  $\text{CaF}_2$  crystal of highest available quality was cleaved along its (111) face in the ultrahigh vacuum at a base pressure of  $2 \times 10^{-8}$  Pa and investigated immediately after preparation. Tips were commercial silicon tips that were used as delivered without any further treatment and cleaning with an undisturbed resonance frequency of 162295.76 Hz and a bending force constant of 42 N/m. The tip radius was roughly estimated to be 10 nm from fitting long-range interaction data as described below. During imaging, the temperature was kept constant at 8 K with a precision of 5 mK, and the cantilever oscillation was stabilized to an amplitude of 6.1 nm. To compensate electrostatic forces, a bias of 0.4–0.9 V was applied between the tip and the metallic sample support. For imaging, the frequency shift was kept constant at  $-25$  Hz, and images represent the error signal of the frequency shift loop; apparent corrugations were typically 20 pm but varied with tip conditions. Images taken at varying tip–sample distances repeatedly showed disk-like contrast typical for a negatively terminated tip.<sup>13</sup> When taking force curves, the feedback loop was switched off and the frequency shift signal was recorded as a function of the reduction in tip–surface distance. Force curves are slightly influenced by piezo creep of the instrument and by thermal drift in the direction perpendicular to the surface. This has been corrected by shifting the experimental frequency shift curves such that the difference of the curves at the set-point for imaging matches the corrugation obtained during imaging. Forces and interaction potentials were obtained from measured frequency shift data using conversion methods described previously.<sup>7,8</sup> The frequency shift was first measured as a function of distance over a large range from 0.5 to 16 nm to evaluate long-range forces (see Figure 1b). The experimental force–distance curve was fitted by a function representing the sum of an electrostatic contribution and a van der Waals contribution acting between a cone with a spherical cap and a flat surface<sup>3,9,10</sup> assuming a Hamaker constant of  $1 \times 10^{-20}$  J and a tip length of 10  $\mu\text{m}$ . The data are measured with a total systematic uncertainty of less than 30%.

Calculations with the Si-based tip were performed using the Linear Combination of Atomic Orbitals (LCAO) basis SIESTA code,<sup>11</sup> which implements the Density Functional Theory and the Generalized Gradient Approximation based on the specific functional of Perdew, Burke, and Ernzerhof. Core electrons are represented by norm-conserving pseudo-

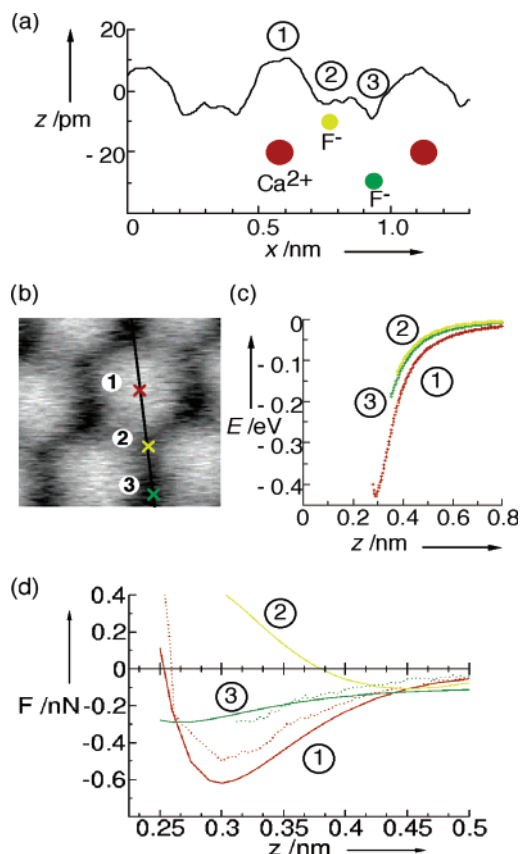


**Figure 2.** Surface topography and site-specific force curves on  $\text{CaF}_2$ (111). Positions above the calcium ion (1), high fluorine ion (2), and low fluorine ion (3) are (a) defined in the cross-section along the  $[211]$  direction ( $x$ -direction) and (b) in a high-resolution image. Note that high and low fluorine positions differ from each other by only 5 pm but are discernible in the image. (d) Experimental force curves (dotted) at positions 1 (red), 2 (light green), and 3 (dark green) compared to theoretical predictions (solid lines) for the respective positions as a function of tip–sample distance  $z$ . (c) Binding energy as a function of tip–sample distance of the tip cluster at positions 1, 2, and 3 derived from the experimental force curves shown in (d).

potentials of the form proposed by Troullier–Martins.<sup>11</sup> We tested many basis sets and found good accuracy with double  $\zeta$  for F, double  $\zeta$  with polarization for Si, H, and O, and triple  $\zeta$  with double polarization for Ca. The top half of the tip and the bottom third of the surface were kept frozen, and all other ions on the tip and on the sample were allowed to relax freely to less than 0.5 eV/nm. The force as a function of tip–surface distance was calculated for discrete values and fitted with a polynomial for easier comparison to experimental curves. Details of the tip–surface calculation method can be found in ref 12.

## Results

In measurements and simulations, we studied interaction potentials above different ionic sites defined in Figure 2a and b. Force curves were taken exactly above the center of the  $\text{Ca}^{2+}$  site (position 1) and at two inequivalent high symmetry sites equidistant from the  $\text{Ca}^{2+}$  ions (positions 2 and 3). The measurement started with a careful approach above sites 2 and 3 and was stopped when reaching the maximum attractive force to avoid tip instability upon further approach. Thereafter, the measurement was repeated above site 1, where the tip was approached 60 pm closer to the surface. Results for the distance-dependent bonding potential curves derived from force curves at all sites are compiled in Figure 2c. Curve 1 differs significantly from the others, demonstrating site-specific binding

- (4) Hug, H. J.; Stiefel, B.; van Schendel, P. J. A.; Moser, A.; Martin, S.; Güntherodt, H. J. *Rev. Sci. Instrum.* **1999**, *70*, 3625.
- (5) Lantz, M. A.; Hug, H. J.; Hoffmann, R.; van Schendel, P. J. A.; Kappenberger, P.; Martin, S.; Baratoff, A.; Güntherodt, H. J. *Science* **2001**, *291*, 2580.
- (6) Barth, C.; Foster, A. S.; Reichling, M.; Shluger, A. L. *J. Phys.: Condens. Matter* **2001**, *13*, 2061.
- (7) Giessibl, F. J. *Appl. Phys. Lett.* **2001**, *78*, 123.
- (8) Pfeiffer, O.; Binnewitz, R.; Baratoff, A.; Meyer, E.; Grütter, P. *Phys. Rev. B* **2002**, *65*, 161403.
- (9) Argento, C.; French, R. H. *J. Appl. Phys.* **1996**, *80*, 6081.
- (10) Hudlet, S.; Jean, M. S.; Guthmann, C.; Berger, J. *Eur. Phys. J. B Condens. Matter* **1998**, *2*, 5.
- (11) Soler, J. M.; Artacho, E.; Gale, J. D.; Garcia, A.; Junquera, J.; Ordejon, P.; Sanchez-Portal, D. *J. Phys.: Condens. Matter* **2002**, *14*, 2745.
- (12) Foster, A. S.; Gal, A. Y.; Airaksinen, J. M.; Pakarinen, O. H.; Lee, Y. J.; Gale, J. D.; Shluger, A. L.; Nieminen, R. M. *Phys. Rev. B* **2003**, *68*, 195420.
- (13) Foster, A. S.; Barth, C.; Shluger, A. L.; Nieminen, R. M.; Reichling, M. *Phys. Rev. B* **2002**, *66*, 235417.

properties. Above the  $\text{Ca}^{2+}$  site, we determine a binding energy of 0.43 eV. From the measured image shown in Figure 2b, the two inequivalent fluorine sites 2 and 3 can clearly be discerned. Residual thermal drift of the apparatus, however, prevents the subtle differences between these two positions from unambiguously being resolved in force curves. The comparison of experiment and theory allows an absolute calibration of the tip–surface distance for the experimental data. As displayed in Figure 2d, the experimental force curves have been shifted along the distance axis so that the minima of experimental and theoretical curves determined above position 1 coincide.

Although we are sure about the nature of positions 1, 2, and 3, the physical meaning of the force and potential energy curves presented in Figure 2 remains unclear unless the structure of the tip apex responsible for the short-range interactions is defined. We performed model calculations assuming different tip configurations, namely, a MgO cluster as used in previous calculations,<sup>6,13</sup> a silicon cluster with hydrogen-saturated dangling bonds, a silicon cluster terminated by an oxygen atom (a characteristic defect on the silica surface<sup>14</sup>), and a hydrogen-saturated  $\text{SiO}_2$  cluster. We found that, for the quantitative comparison required in this work, the MgO cluster is not the best tip model as it overestimates the binding energy due to the large polarity of MgO. We also dismissed the model of a pure silicon tip as the respective simulations cannot reproduce the experimentally observed circular image contrast pattern. This is an expected result as the tip used in our experiments was exposed to air and, therefore, covered by native oxide. As a more appropriate tip model, we identified the structure of a hydrogen-saturated silicon tip terminated by a single oxygen atom, as it provides scan lines characteristic of disk-like contrast and forces comparable to experiment. Force curves calculated for this tip model at positions 1, 2, and 3 are shown in Figure 2d. In agreement with the experiment, we find a maximum attractive force of about 600 pN above the  $\text{Ca}^{2+}$  ion, while forces are smaller above the fluorine ions. Note also the excellent agreement in shape of the maximum curve of position 1, indicating that the simulations are capturing the dominant atomic processes and interactions in the experiment. However, while the experimental curves are reproduced for the calcium 1 and fluorine 3 positions, there is an obvious deviation for the fluorine 2 position. The calculated force curves predict repulsion in a region where the experiment clearly yields attraction.

## Discussion

We explored this question by calculating force curves assuming a tip cluster composed of  $\text{SiO}_2$  with dangling bonds saturated by hydrogen. Due to the more complex structure of this cluster, instead of one atom clearly protruding and dominating the interaction with the surface, other atoms may contribute significantly to the chemical interaction.<sup>15</sup> This becomes immediately evident from the comparison of simulation results for the tip approach series reproduced in Figure 3a–c and d–f, representing results for both tip models. Above position 2, for the simple, oxygen-terminated silicon tip, the oxygen mainly experiences repulsion from the high fluorine, causing significant inward relaxation of this ion. For the silica tip cluster, there is

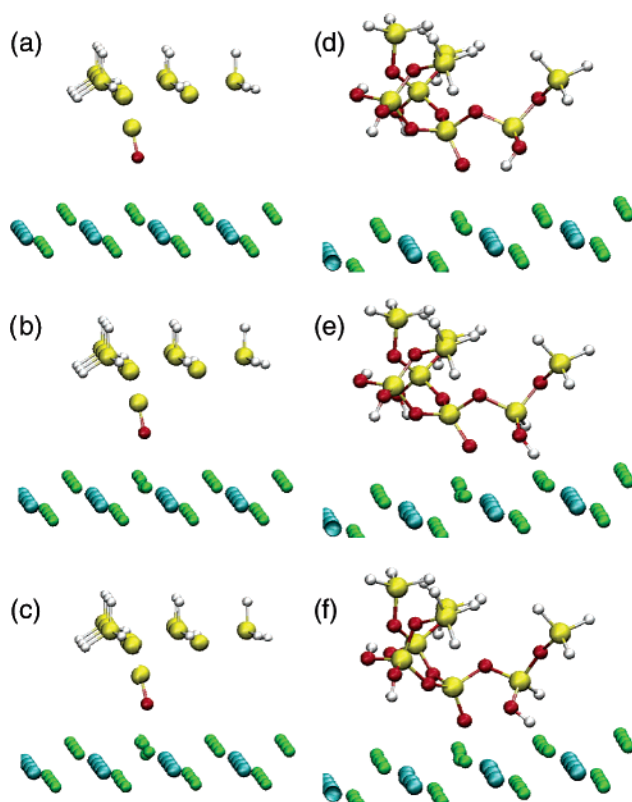


**Figure 3.** Simulations demonstrating atomic relaxation of tip and surface atoms during approach of the tip to the  $\text{CaF}_2(111)$  surface above the high fluorine ion (position 2). Model tips are a hydrogen-saturated Si tip with a single oxygen atom at the end in (a), (b), and (c), and a  $\text{SiO}_2$  tip with hydrogen-saturated dangling bonds in (d), (e), and (f). Images shown are snapshots taken from a series of calculations for varied tip–surface distance: (a)  $z = 375$  pm, (b)  $z = 340$  pm, (c)  $z = 300$  pm, and (d)  $z = 375$  pm, (e)  $z = 300$  pm, (f)  $z = 240$  pm. Distance values given represent the distance between the foremost oxygen atom and the plane of  $\text{Ca}^{2+}$  ions. Series a–c demonstrate strongly repulsive interaction between the tip-terminating oxygen and the high fluorine ion, resulting in an inward relaxation of the ion. In series d–f, there is an additional attractive interaction upon close approach between the foremost hydrogen atom that is strongly pulled towards the nearest neighbor high fluorine ion.

an additional attractive interaction of the most protruding hydrogen atom with the neighboring high fluorine, and the overall interaction between tip cluster and surface is attractive, although the interaction between the tip-terminating oxygen and the adjacent high fluorine is clearly repulsive. Note that the asymmetry expected in the imaging due to this additional interaction cannot be detected in images as they are taken at larger tip–surface distance. Calculating a force curve for this silica tip yields, in fact, a shallow minimum in a region where we find repulsion for the oxygen-terminated silicon tip and thus a possible explanation for our experimental finding of similar force curves above low and high fluorines. The increased interaction with the surface provided by the additional ions on the silica tip near the surface means that the absolute magnitude of forces is larger than that in the experiment.<sup>16</sup> However, the calculations shown here demonstrate the general principle that less ideal tips can easily explain the lack of repulsion in experiments, and a further, very extensive study of different tips is likely to provide complete agreement.

(14) Ma, Y.; Foster, A. S.; Nieminen, R. M. *J. Chem. Phys.* **2005**, *122*, 144709.

(15) Hoffmann, R.; Lantz, M. A.; Hug, H. J.; Van Schendel, P. J. A.; Kappenberger, P.; Martin, S.; Baratoff, A.; Güntherodt, H. J. *Phys. Rev. B* **2003**, *67*, 085402.

(16) Foster, A. S.; Shluger, A. L.; Nieminen, R. M. *Nanotechnology* **2004**, *15*, S60.

## Conclusion

Case studies based on combined efforts in experiment and theory such as the one presented here yield deep insight into the complex interactions of a molecular cluster with a surface. The methods and concepts developed here can be transferred to more general situations of cluster–surface interaction and provide a high degree of quantitative understanding of chemical bond formation between cluster atoms and *specific surface sites*. Previous single bond studies have been restricted to identifying one covalent bond in a series of bond breaking events during rupture of extended molecules.<sup>17</sup> Here, we are able to specifically address bonds, clarify their role in the interaction of a cluster with a surface, and quantitatively measure the interaction. This could be used to identify specific surface sites on a general surface. The task of identifying surface atoms becomes simpler and more reliable if one can choose certain particular points that should be significantly different from one another where measurements are carried out. In the case of CaF<sub>2</sub>, these are the Ca<sup>2+</sup> positions and two different F<sup>-</sup> positions in contrast to a system with NaCl structure, where there are only two particular points. Another route is to choose points on the surface where tip relaxation is minimal for symmetry reasons, and the results therefore become independent of the chemical nature and position of most of the tip atoms.<sup>18</sup> Measuring above specific surface sites also greatly helps to identify the atomic structure

at the tip end in future force microscopy experiments. This approach can further be extended by using the site-selectively measured energy dissipation to which we have access by measuring the cantilever excitation amplitude. We expect this channel to be even more sensitive to the chemical nature of the tip.<sup>19</sup> This approach paves the way to a direct, site-selective measurement of binding forces of molecules to surfaces by placing them at the end of the tip of a force microscope. Further development of this approach will provide new insight into mechanisms of chemical bond formation between clusters, cluster deposition at surfaces, processes in adhesion and tribology, and single atom manipulation with the force microscope.<sup>20,21</sup>

**Acknowledgment.** The authors would like to thank the Swiss National Center of Competence in Research “Nanoscale Science” for supporting the measurements shown in this article. R.H. is grateful to the German DFG-Center for Functional Nanostructures, Karlsruhe, for funding. A.S.F. is grateful to the Academy of Finland for funding and to the Centre for Scientific Computing, Helsinki, for computational resources.

**Supporting Information Available:** Additional larger SFM images (PDF). This material is available free of charge via the Internet at <http://pubs.acs.org>.

JA055267I

- (17) Grandbois, M.; Beyer, M.; Rief, M.; Clausen-Schaumann, H.; Gaub, H. E. *Science* **1999**, *283*, 1727.  
(18) Hoffmann, R.; Kantorovich, L. N.; Baratoff, A.; Hug, H. J.; Güntherodt, H. J. *Phys. Rev. Lett.* **2004**, *92*, 146103.

- (19) Trevelyan, T.; Kantorovich, L. N. *Nanotechnology* **2005**, accepted.  
(20) Oyabu, N.; Custance, O.; Yi, I.; Sugawara, Y.; Morita, S. *Phys. Rev. Lett.* **2003**, *90*, 176102.  
(21) Sugimoto, Y.; Abe, M.; Hirayama, S.; Oyabu, N.; Custance, O.; Morita, S. *Nat. Mater.* **2005**, *4*, 156.